Frequency-Selective Joint Tx/Rx I/Q Imbalance Estimation Using Golay Complementary Sequences

R. Rodríguez-Ávila, G. Núñez-Vega, R. Parra-Michel, and A. Mendez-Vazquez

***Abstract*—The increasing use of smaller technologies in the manufacture of analog front–ends (AFEs) for communication systems has increased the impact their non–ideal components produce. This results in a significant degradation of the system performance that must be identified and addressed. In particular, the I/Q imbalance is commonly estimated and compensated via digital signal processing techniques using training sequences. In order to preclude the rise of other non–idealities, such as the non–linearity of the power amplifier (PA), these training sequences should be chosen to have a low peak–to–average power ratio (PAPR). In addition, it is desirable that these techniques have reduced computational complexity for minimizing estimation times and area resources.**

This paper presents a novel I/Q imbalance estimation algorithm that is computationally simple, it only requires adders and shifters, while exhibiting a PAPR ≤ 2. It can include the transmitter and receiver I/Q imbalances as well as the multipath phenomena. It is based on a newly used property of Golay complementary sequences (GCS). The statistical efficiency and low complexity of the proposed algorithm are proved, while its flexibility is illustrated under several extreme test cases.

***Index Terms*—Golay complementary sequences, I/Q imbalance, OFDM.**

I. Introduction

THE use of high–performance wireless communications systems is continuously growing. The tendency is to use the newest (smallest) technologies in the manufacturing process because they make possible to incorporate more functionality in the same silicon area. These technologies allow higher throughputs, but at the same time, problems that used to be insignificant become evident now. One of these problems is that the manufactured analog components behave far from their ideal functionality. Particularly, the AFE suffers from the so–called In–phase and Quadrature–phase (I/Q) imbalance. This is defined as a difference between the gains, phases and even impulse responses of the filters on each orthogonal branch of a radio communication system (RCS). This causes the loss of the required orthogonality property. Furthermore, this situation is aggravated by the fact that modern RCSs rely on the zero intermediate–frequency (Zero IF) approach due to its high flexibility, relatively low cost and low power consumption. In these systems, any I/Q imbalance produces a high degree of self–interference [1]. In the case of orthogonal–frequency division multiplexing (OFDM) systems, which are becoming the de–facto standard for RCS, the I/Q imbalance produces inter–carrier interference (ICI) that severely limits the system performance [2], [3]. Furthermore, complex I/Q mixing is carried out both in the transmitter (Tx) and the receiver (Rx). Thus, there may be two independent contributions to signal distortion in addition to the propagation channel [2], [4].

Although the origin of this problem appears in the analog domain, it is preferable to deal with it using digital algorithms rather than increase the cost of analog components and re–designing a complete new AFE [2], as is extensively found in the open literature. Particularly, in [5] and [6], a base–band (BB) model for the frequency–selective (FS) Tx I/Q imbalance is presented. In addition, [6] presents the BB model for the FS Rx I/Q imbalance. In [4] and [7], a BB model considers the frequency–independent (FI) Tx and Rx I/Q imbalances, as well as the multipath phenomena. In [7] it is also presented a BB model that considers FI Tx I/Q imbalance, multipath phenomena and FS Rx I/Q imbalance.

Concerning the estimation and compensation schemes of these models, two main approaches can be found: the blind approach [3], [5] and the trained approach [4], [8], [9], [10]. The first one considers the statistical properties of the transmitted data, while the second one considers the transmission of training sequences. As the non–trained approaches require complex hardware and a large amount of time to produce reliable results, they will not be examined in this paper.

Regarding training methods, it is proposed in [8] a set of complex–valued training sequences that are optimum in the sense of having PAPR = 1. By using these sequences, a general widely–linear system (WLS), which models the I/Q imbalance, is estimated via the multiplication of the inverse of a well–conditioned matrix times the received samples. Although these sequences discard the non–linearities caused by the PA, the estimation algorithm exhibits an $O(N^2)$ complexity. In [4] it is presented an iterative method used to sequentially estimate first the multipath phenomena, second the FI Rx I/Q imbalance and third the FI Tx I/Q imbalance by using the pilots in an OFDM frame. However, this sequentially refined estimation and compensation of the overall I/Q imbalance and multipath phenomena requires a large amount of processing time and involves a $O(N^2)$ complexity. Another FS overall I/Q imbalance estimation approach, commonly used in practice, consists of the transmission of a pair of tones (sinusoids)

Manuscript received May 4, 2012; revised November 17, 2012; accepted February 21, 2013. The associate editor coordinating the review of this paper and approving it for publication was Y. Mao.

This work was supported by INTEL research grant DAIR-2011 and CONACYT research grant 181962.

The authers are with the Department of Electrical Engineering, Communications Section, CINVESTAV-IPN; Av. del Bosque 1145, Col. El Bajio, 45019, Zapopan, Jalisco, Mexico (e-mail: {ravila, gnunez, rparra, amendez}@gdl.cinvestav.mx).

Digital Object Identifier 10.1109/TWC.2013.040213.120622

that test a single pair of mirror frequencies in the system bandwidth. Therefore, from the received signal, a set of equations can be stated and solved. For the FS I/Q imbalance case, this approach has the following implications: it requires a large amount of time, as N sets of sequences has to be sent for estimating N frequency points. Furthermore, when several tones are sent in each sequence (multi–tones), the PAPR could be as much as N [11], causing the PA to introduce non–linearities into the model. As a result, unreliable estimations are produced.

As for the hardware implications, two important features are preferred for an efficient estimation algorithm. The first one is that it should reuse the already–built hardware module components of a RCS, while the second one is that it should involve simple mathematical expressions that translate into easy–to–implement hardware modules.

This paper addresses the topic of a low–complexity algorithm for estimating the parameters of a model that can include the FS Tx I/Q imbalance, multipath phenomena and the FS Rx I/Q imbalance by using training sequences. The proposed approach relaxes the choice of the optimum sequences for PAPR purposes. Instead, it uses GCS which yield good PAPR, while at the same time reducing hardware implications and computational complexity. These sequences are commonly used in spread spectrum techniques, radar, Hadamard matrices construction and linear systems identification [12], [13], [14].

A. Objectives and contributions

The aim of this paper is to provide a low complexity estimation algorithm for the FS I/Q imbalance problem. Two contributions are provided to achieve the goal. The first one is a general model that incorporates all parameters involved in the complete FS I/Q imbalance problem. These parameters include the FS I/Q imbalance at Tx, multipath propagation channel and the FS I/Q imbalance at Rx and their combinations. The second contribution, and the most important, is the introduction of a newly used property of the GCS which makes them useful for devising an efficient estimation algorithm suitable for all cases of I/Q imbalances. This proposed estimation algorithm is efficient in statistical sense while at the same time, it exhibits a complexity of *O(N)*. In addition, the PAPR of the used training sequences is close to the optimum. It should be pointed out that the aforementioned property of the GCS is not the well–known property that the sum of their auto–correlations equals the delta function [14], but a different one related to the sum of their Hadamard products.

B. Notations

Upper case letters denote frequency–domain signals; lower case letters denote time–domain signals; $(\cdot)^*$ denotes complex conjugate; $*$ and $\odot$ denote convolution and Hadamard product respectively; $E\{\cdot\}$ denotes the expectation operator. The main acronyms are: AWGN (additive white Gaussian noise); BB (base–band); DFT (discrete–Fourier transform); FI (frequency–independent); FS (frequency–selective); GCS (Golay complementary sequences); LPF (low–pass filter); I/Q (In–phase and Quadrature–phase); OFDM (orthogonal–frequency division multiplexing); PAPR (peak–to–average power ratio); Rx (receiver); Tx (transmitter); WLS (widely–linear system).

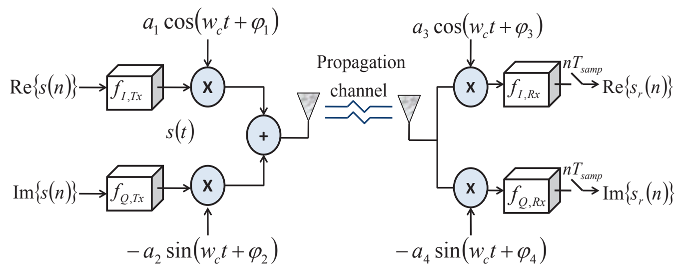

Fig. 1. General I/Q mixing scheme.

C. Organization

The structure of this article is as follows: Section II presents the general mathematical models describing the I/Q imbalance and the effects of this problem. Section III proposes an estimation algorithm based on the newly used GCS property, and its performance is analyzed in Section IV. Section V shows the performance of the proposed algorithm by simulating an OFDM system under several I/Q imbalance cases. Finally, the conclusions are stated in Section VI.

II. IQ Imbalance Models

The general I/Q mixing system model is shown in Fig. 1, where $s(n)$ is the complex-valued discrete BB data signal, $s(t)$ is the continuous data signal and $s_r(n)$ is the received discrete BB data signal. Considering that the LPFs and multipath phenomena are modeled in the discrete–time domain as discrete finite impulse response (FIR) filters, $h(n)$ can be defined as the discrete–time representation of the propagation channel, $f_{I,Tx}(n)$ and $f_{Q,Tx}(n)$ are the LPFs that model the differences between the nominal responses at the corresponding I and Q branches in Tx and $f_{I,Rx}(n)$ and $f_{Q,Rx}(n)$ in Rx. In addition, the following terms are defined:

$$
\begin{aligned}
\gamma_{Tx}(n) &= \frac{f_{I,Tx}(n)+g_{Tx}e^{j\varphi_{Tx}}f_{Q,Tx}(n)}{2},\\
\beta_{Tx}(n) &= \frac{f_{I,Tx}(n)-g_{Tx}e^{j\varphi_{Tx}}f_{Q,Tx}(n)}{2},\\
\gamma_{Rx}(n) &= \frac{f_{I,Rx}(n)+g_{Rx}e^{-j\varphi_{Rx}}f_{Q,Rx}(n)}{2},\\
\beta_{Rx}(n) &= \frac{f_{I,Rx}(n)-g_{Rx}e^{j\varphi_{Rx}}f_{Q,Rx}(n)}{2};
\end{aligned}
\tag{1}
$$

where $g_{Tx} = \frac{a_2}{a_1}$ and $g_{Rx} = \frac{a_4}{a_3}$ are the gain imbalances at Tx and Rx respectively. $\varphi_{Tx} = \phi_2 - \phi_1$ and $\varphi_{Rx} = \phi_4 - \phi_3$ are the phase imbalances in Tx and Rx respectively [4]. From the general system model in Fig. 1, it follows, by means of the definitions mentioned previously and certain mathematical calculations, that the received signal can be expressed as:

$$
\begin{aligned}
s_r(n) =&\\
&(\gamma_{Tx}(n) * \gamma_{Rx}(n) * h(n) + \beta^*_{Tx}(n) * \beta_{Rx}(n) * h^*(n)) * s(n)\\
&+(\gamma_{Rx}(n) * \beta_{Tx}(n) * h(n) + \beta_{Rx}(n) * \gamma^*_{Tx}(n) * h^*(n)) * s^*(n)\\
&+\gamma_{Rx}(n) * \eta(n) + \beta_{Rx}(n) * \eta^*(n),
\end{aligned}
\tag{2}
$$

where $\eta(n)$ is the discrete complex low-pass representation (BB representation) of the AWGN encountered at the low-noise amplifier (LNA) in the Rx. For simplicity, (2) can be reduced to:

$$
s_r(n) = \gamma(n) * s(n) + \beta(n) * s^*(n) + \epsilon(n), \tag{3}
$$

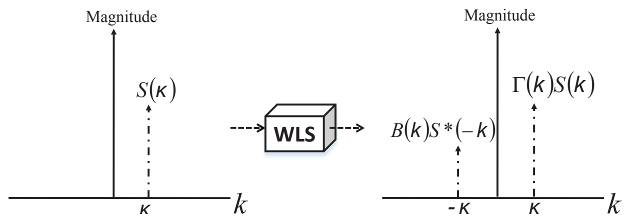

Fig. 2. Effect of a WLS defined by $\Gamma(\kappa)$ and $B(\kappa)$ over a single tone, $S(\kappa)$, centered in the κ-th frequency.

where $\gamma(n) = \gamma_{Tx}(n) * \gamma_{Rx}(n) * h(n) + \beta^*_{Tx}(n) * \beta_{Rx}(n) * h^*(n)$ and $\beta(n) = \gamma_{Rx}(n) * \beta_{Tx}(n) * h(n) + \beta_{Rx}(n) * \gamma^*_{Tx}(n) * h^*(n)$ are the FIR filters that incorporate the FS parameters of Tx LPFs, the multipath propagation channel and Rx LPFs. In addition, $\epsilon(n) = \gamma_{Rx}(n) * \eta(n) + \beta_{Rx}(n) * \eta^*(n)$ is the term containing the colored noise. In this and the following section, the term $\epsilon(n)$ will be omitted to ease explanation of the proposed estimation algorithm; however it will be treated in detail in section IV, where the statistical analysis of the estimator is carried out.

The orthogonality property between I/Q branches is very important for recovering the information on each of them without mutual interference. This implies that Tx gains $a_1 = a_2$, Tx phases $\phi_1 = \phi_2$, Tx LPFs $F_{I,Tx} = F_{Q,Tx}$; Rx gains $a_3 = a_4$, Rx phases $\phi_3 = \phi_4$ and Rx LPFs $F_{I,Rx} = F_{Q,Rx}$. In this case, $s_r(n) = s(n)$.

In the case when there are some gain or phase differences between orthogonal branches at either the Tx or Rx, the so–called I/Q imbalance problem arises causing the branches to interfere with each other. Viewing the received signal in the frequency domain provides an easy way to understand how the I/Q imbalances distort the received signal. Applying the DFT to (3) and (1), it results in:

$$S_r(k) = \Gamma(k)S(k) + B(k)S^*(-k), \tag{4}$$

and

$$\begin{aligned} \Gamma_{Tx}(k) &= \frac{F_{I,Tx}(k) + g_{Tx}e^{j\varphi_{Tx}}F_{Q,Tx}(k)}{2}, \\ B_{Tx}(k) &= \frac{F_{I,Tx}(k) - g_{Tx}e^{j\varphi_{Tx}}F_{Q,Tx}(k)}{2}, \\ \Gamma_{Rx}(k) &= \frac{F_{I,Rx}(k) + g_{Rx}e^{-j\varphi_{Rx}}F_{Q,Rx}(k)}{2}, \\ B_{Rx}(k) &= \frac{F_{I,Rx}(k) - g_{Rx}e^{j\varphi_{Rx}}F_{Q,Rx}(k)}{2}; \end{aligned} \tag{5}$$

where $S(k)$, $S_r(k)$, $\Gamma(k)$, $B(k)$, $\Gamma_{Tx}(k)$, $\Gamma_{Rx}(k)$, $B_{Tx}(k)$ and $B_{Rx}(k)$ are the corresponding DFTs of $s(n)$, $s_r(n)$, $\gamma(n)$, $\beta(n)$, $\gamma_{Tx}(n)$, $\gamma_{Rx}(n)$, $\beta_{Tx}(n)$, $\beta_{Rx}(n)$. In particular, k is an indexing variable for the frequency components such that $-\frac{N}{2} \le k \le \frac{N}{2} - 1$, and N is the number of DFT points considered as an even number without loss of generality.

Equations (3) and (4), in fact, have the structure of a so–called WLS [15]. In order to see the effect of the WLS over a band–limited signal (i.e. the effect of the I/Q imbalance), suppose now that $S(\kappa)$ is a single tone located at κ-th frequency. Applying it to (4) results in a signal that contains two tones located at κ-th and $-\kappa$-th frequencies, weighted by $\Gamma(\kappa)$ and $B(\kappa)$ respectively, as shown in Fig. 2.

Following this reasoning, it is easy to infer that each spectral component of the BB signal will produce a weighted self–interference to its "mirror" frequency, leading to a significant performance degradation.

From (4) and (5), note that when Tx is considered as ideal, i.e., there are no mismatches between orthogonal branches at Tx, then $\Gamma_{Tx}(k) = F_{I,Tx}(k) = F_{Q,Tx}(k)$ $\forall k$ and $B_{Tx}(k) = 0$ $\forall k$. However, the remaining problems like Rx I/Q imbalances (with/without considering propagation channel) maintain the model as a WLS. Considering now that Rx is ideal, it means that $\Gamma_{Rx}(k) = F_{I,Rx}(k) = F_{Q,Rx}(k)$ $\forall k$ and $B_{Rx}(k) = 0$ $\forall k$, and the previous observation is maintained. Even when there are no I/Q imbalances at Tx and Rx and the impulse responses of the LPF are ideal ($F_{I,Tx}(k) = F_{Q,Tx}(k) = F_{I,Rx}(k) = F_{Q,Rx}(k) = 1 \forall k$), the propagation channel can be represented by a WLS with $\Gamma(K) = H(k)$ and $B(k) = 0$ $\forall k$. Thus, all the combinations of I/Q imbalances and propagation channel models can be integrated into an adequate WLS.

A. A well-known compensation scheme

It is known that the received signal is distorted by the WLS model. In order to avoid this distortion, a popular method uses the estimation of the complex imbalance factors $\Gamma(k)$ and $B(k)$ instead of the individual non–idealities (g_{Tx}, g_{Rx}, etc.). When the complex imbalance factors are obtained, a distortion (pre-distortion) scheme can be applied to the transmitted signal in order to eliminate the I/Q imbalance issues, independently of which non–idealities have caused these imbalance factors.

As an example of how a WLS can be compensated, consider the case of a FI I/Q imbalance model either at Tx or Rx. From (4) and its conjugate and flipped version, the following matrix equation can be formulated:

$$\begin{bmatrix} S_r(k) \\ S^*_r(-k) \end{bmatrix} = \begin{bmatrix} \Gamma & B \\ B^* & \Gamma^* \end{bmatrix} \begin{bmatrix} S(k) \\ S^*(-k) \end{bmatrix} = \mathbf{D} \begin{bmatrix} S(k) \\ S^*(-k) \end{bmatrix} \tag{6}$$

The original BB signal can be recovered by finding the inverse of the distortion matrix $\mathbf{D}$. Using the determinant, the compensator is defined by the following equation:

$$S(k) = F_1 S_r(k) + F_2 S^*_r(-k), \tag{7}$$

where the compensation factors F_1 and F_2 are defined as [3]:

$$\begin{aligned} F_1 &= \frac{\Gamma^*}{|\Gamma|^2 - |B|^2}, \\ F_2 &= \frac{-B}{|\Gamma|^2 - |B|^2}. \end{aligned} \tag{8}$$

When the idea is extended to a FS model, similar reasoning can be used. Then the obtained compensation factors for the k-th frequency component are the following:

$$\begin{aligned} F_1(k) &= \frac{\Gamma^*(-k)}{\Gamma(k)\Gamma^*(-k) - B(k)B^*(-k)}, \\ F_2(k) &= \frac{-B(k)}{\Gamma(k)\Gamma^*(-k) - B(k)B^*(-k)}. \end{aligned} \tag{9}$$

Note that these factors can be used in a pre–distortion scheme, which consists in applying them to the signal to be transmitted producing the same total effect over the received signal.

III. Proposed Estimation Algorithm

The general model for the I/Q imbalance problem has been defined in (4) by using the imbalance factors in (5). This paper considers the estimation of the imbalance factors $\Gamma(k)$ and $B(k)$ using the GCS as frequency-domain training sequences due to a particular property explained in the next subsection.

A. Golay complementary sequences

The Golay complementary sequences were introduced by Marcel J. Golay in 1949 in the context of infrared spectrometry. The best–known property of these sequences is that their out-of-phase aperiodic auto–correlation coefficients add up to zero [14]. As a consequence of this property, time-domain GCS are widely used for linear system estimations such as single-input single-output (SISO) and multiple-input multiple-output (MIMO) radar target detection [16] and BB channel estimation for wireless communication standards such as the recently defined 60 Ghz standard [17]. Besides these applications, GCS have been used in some other areas in telecommunications such as coded ultrasound imaging systems [18], OFDM coding schemes for PAPR control [19] and Hadamard matrices construction [13]. In addition, there are a few works related to the use of GCSs to estimate a linear channel with some third-order weak non–linearity [20]. It is worth mentioning that these sequences have not been used for the estimation of the particular case of non–linear systems that model the I/Q imbalance, specifically WLSs.

In his paper, Golay defined L-length complementary sequences $S_{aL}(n)$ and $S_{bL}(n)$, whose elements $S_a(i)$, $S_b(i)$ $\in \{1, -1\}$, as a pair of sequences in which the number of pairs of equal elements with any given position distance greater or equal to 1 in one series is equal to the number of unequal elements with the same position distance in the other series [21]. From the same work, it can be highlighted that this definition is equivalent to the following mathematical expression:

$$S_{aL}(r) + S_{aL}(L-r-1) + S_{bL}(r) + S_{bL}(L-r-1) = 1(mod2);\quad r = 0 \dots \tfrac{L}{2} - 1. \tag{10}$$

The interpretation of (10) is that three of the four elements $S_{aL}(r)$, $S_{aL}(L-r-1)$, $S_{bL}(r)$ and $S_{bL}(L-r-1)$ have the same sign. Based on this interpretation, equation (11) follows directly from (10):

$$S_{aL}(r)S_{aL}(L-r-1) + S_{bL}(r)S_{bL}(L-r-1) = 0,\quad r = 0 \dots \tfrac{L}{2} - 1; \tag{11}$$

which in turn, leads directly to the well–known auto–correlation property. This property can be easily derived based on the following observation: every given position distance corresponds to the same delay in the auto–correlation function and when the indexing variable r is swept over all possible values and the summation is performed, (11) becomes:

$$\begin{gathered}\textstyle\sum_{r=0}^{N-n-1} S_{aL}(r)S_{aL}(n+r) + \sum_{r=0}^{N-n-1} S_{bL}(r)S_{bL}(n+r) = 0,\\ for \qquad n \neq 0;\\ \textstyle\sum_{r=0}^{N-n-1} S_{aL}(r)S_{aL}(n+r) + \sum_{r=0}^{N-n-1} S_{bL}(r)S_{bL}(n+r) = 2N,\\ for \qquad n = 0.\end{gathered} \tag{12}$$

Although (12) is the most–cited property of GCS, there is another interpretation to (10) and (11) in terms of the Hadamard products. The series $S_{aL}(L-r-1)$ and $S_{bL}(L-r-1)$ with $r = 0 \dots L-1$ are the flipped (inverted in time) versions of the series $S_{aL}(r)$ and $S_{bL}(r)$ respectively. For convenience, the flipped version of $S_{xL}(n)$ will be denoted as $S'_{xL}(n)$. Then (11) can be stated in terms of the Hadamard products of these sequences as:

$$S_{aL}(n) \odot S'_{aL}(n) + S_{bL}(n) \odot S'_{bL}(n) = 0_L. \tag{13}$$

Furthermore, taking into account (10) and (11) again:

$$S_{aL}(n) \odot S'_{bL}(n) + S_{bL}(n) \odot S'_{aL}(n) = 0_L. \tag{14}$$

From the previous discussion, it is possible to introduce the following properties:

$$\begin{gathered}S_{aL}(n) \odot S'_{aL}(n) + S_{bL}(n) \odot S'_{bL}(n) = 0_L,\\ S_{aL}(n) \odot S'_{bL}(n) + S_{bL}(n) \odot S'_{aL}(n) = 0_L,\\ S_{aL}(n) \odot S_{aL}(n) + S_{bL}(n) \odot S_{bL}(n) = 2_L.\end{gathered} \tag{15}$$

The three expressions in (15) represent a useful tool for devising a new estimation algorithm for WLSs.

B. Algorithm explanation

The properties in (15), to the best of the authors' knowledge, have not been used before in the context of WLS estimation. On the basis of these properties, the GCS can be used as frequency–domain training sequences for estimating the component parameters of the WLS by solving a system of equations efficiently. First, substituting $S(k)$ in (4) with an N–length pair of GCS, $S_a(k)$ and $S_b(k)$ results in:

$$\begin{aligned}S_{ra}(k) &= \Gamma(k)S_a(k) + B(k)S_a^*(-k),\\ S_{rb}(k) &= \Gamma(k)S_b(k) + B(k)S_b^*(-k);\end{aligned} \tag{16}$$

where $S_{ra}(k)$ and $S_{rb}(k)$ are the frequency–domain received signals corresponding to each sequence of the pair of GCS. Knowing that the GCS are binary phase shift keying (BPSK), the conjugation has no effect on them. Finally, using this idea, (11) becomes:

$$\begin{aligned}S_{ra}(k) &= \Gamma(k)S_a(k) + B(k)S'_a(k),\\ S_{rb}(k) &= \Gamma(k)S_b(k) + B(k)S'_b(k),\end{aligned} \tag{17}$$

where $S_a(-k) = S'_a(k)$ and $S_b(-k) = S'_b(k)$ are the flipped versions of the GCS. Considering that carrier frequency offset was previously addressed by an adequate correction algorithm, then $C_a(k)$ and $C_b(k)$ can be defined as the Hadamard products between the received signal and its corresponding component of the GCS, as in:

$$\begin{aligned}C_a(k) &= S_{ra}(k) \odot S_a(k),\\ C_b(k) &= S_{rb}(k) \odot S_b(k).\end{aligned} \tag{18}$$

Then, the sum of $C_a(k)$ and $C_b(k)$ results in:

$$\begin{gathered}C_a(k) + C_b(k) =\\ \Gamma(k)[S_a(k) \odot S_a(k) + S_b(k) \odot S_b(k)]\\ +B(k)[S'_a(k) \odot S_a(k) + S'_b(k) \odot S_b(k)],\\ = 2\Gamma(k).\end{gathered} \tag{19}$$

Note that (15) was required in the derivation of (19). Note also that (19) consists of very simple operations, which allows for the estimation of one of the parameters of the WLS ($\Gamma(k)$). The other parameter component of the WLS, $B(k)$, can be estimated in a similar way, i.e., by defining $D_a(k)$ and $D_b(k)$ as the Hadamard products between the received signal and its corresponding flipped component of the GCS, as in:

$$\begin{aligned}D_a(k) = S_{ra}(k) \odot S'_a(k),\\ D_b(k) = S_{rb}(k) \odot S'_b(k),\end{aligned} \tag{20}$$

and the sum of $D_a(k)$ and $D_b(k)$ leads to:

$$\begin{array}{c} D_a(k) + D_b(k) \\ = \Gamma(k)[S_a(k) \odot S'_a(k) + S_b(k) \odot S'_b(k)] \\ +B(k)[S_a(k) \odot S_a(k) + S_b(k) \odot S_b(k)], \\ = 2B(k). \end{array} \tag{21}$$

As a result of equations (19) and (21), the WLS parameters are obtained as follows:

$$\begin{array}{rcl} \Gamma(k) & = & \frac{1}{2}\{S_{ra}(k) \odot S_a(k) + S_{rb}(k) \odot S_b(k)\}, \\ B(k) & = & \frac{1}{2}\{S_{ra}(k) \odot S'_a(k) + S_{rb}(k) \odot S'_b(k)\}. \end{array} \tag{22}$$

IV. Performance Evaluation

A. Statistical analysis

In the presence of noise, the proposed algorithms in (22) becomes estimators, therefore it is mandatory to assess their statistical performance [22]. Hence, the consistence of these estimators will be subsequently discussed. Following the same procedure from (3), but considering now the colored noise, then (16) is expressed as:

$$\begin{array}{rcl} S_{ra}(k) & = & \Gamma(k)S_a(k) + B(k)S^*_a(-k) + W_1(k), \\ S_{rb}(k) & = & \Gamma(k)S_b(k) + B(k)S^*_b(-k) + W_2(k); \end{array} \tag{23}$$

where $W_x(k) = \Gamma_{Rx}(k)N_x(k) + B_{Rx}(k)N^*_x(-k)$ is the DFT of the term $\epsilon(n)$ in (3), i.e. is the noise sequence that results from AWGN, $N_x(k)$, weighted by the receiver's filters $\Gamma_{Rx}(k)$ and $B_{Rx}(k)$ (colored in time) and $x = 1, 2$. Therefore, (22) is changed accordingly to provide an estimation of $\Gamma(k)$ and $B(k)$, denoted as $\hat{\Gamma}(k)$ and $\hat{B}(k)$, respectively. This is obtained by the following equations:

$$\begin{array}{rcl} \hat{\Gamma}(k) & = & \frac{1}{2}\{S_{ra}(k) \odot S_a(k) + S_{rb}(k) \odot S_b(k) + m_1(k)\}, \\ \hat{B}(k) & = & \frac{1}{2}\{S_{ra}(k) \odot S'_a(k) + S_{rb}(k) \odot S'_b(k) + m_2(k)\}, \end{array} \tag{24}$$

where $m_1(k) = S_a(k) \odot W_1(k) + S_b(k) \odot W_2(k)$ and $m_2(k) = S'_a(k) \odot W_1(k) + S'_b(k) \odot W_2(k)$. Selecting the k-th frequency component with $k = \kappa$, the mean of the estimator $\hat{\Gamma}(\kappa)$ can be evaluated explicitly as:

$$\begin{array}{c} E\left\{\hat{\Gamma}(\kappa))\right\} = \\ \frac{1}{2}E\left\{ \begin{array}{l} \left(\Gamma(\kappa)S_a(\kappa) + B(\kappa)S'^*_a(\kappa) + W_1(\kappa)\right) \odot S_a(\kappa) \\ + \left(\Gamma(\kappa)S_b(\kappa) + B(\kappa)S'^*_b(\kappa) + W_2(\kappa)\right) \odot S_b(\kappa) \end{array} \right\}. \end{array} \tag{25}$$

Applying the expectation operator to each term, it results in:

$$\begin{array}{c} E\left\{\hat{\Gamma}(\kappa))\right\} = \\ \frac{1}{2}\left\{ \begin{array}{l} E\{\Gamma(\kappa)\}\varepsilon_a(\kappa) + E\{B(\kappa)\}\varepsilon'_a(\kappa) + E\{W_1(\kappa)\}S_a(\kappa) \\ +E\{\Gamma(\kappa)\}\varepsilon_b(\kappa) + E\{B(\kappa)\}\varepsilon'_b(\kappa) + E\{W_2(\kappa)\}S_b(\kappa) \end{array} \right\}, \end{array} \tag{26}$$

where $\varepsilon_a(\kappa) = S_a(\kappa)S_a(\kappa) = 1$ and $\varepsilon'_a(\kappa) = S'_a(\kappa)S_a(\kappa)$; the same applies for ε_b and ε'_b. Now, taking into account 10, (26) is simplified to:

$$E\left\{\hat{\Gamma}(\kappa)\right\} = \frac{2E\{\Gamma(\kappa)\}}{2} + \frac{S_{aN}(\kappa)E\{W_1(\kappa)\}}{2} + \frac{S_{bN}(\kappa)E\{W_2(\kappa)\}}{2}. \tag{27}$$

Going through the previous steps, it can be shown that $E\left\{\hat{B}(\kappa)\right\}$ results in an expression similar to that in (27). It can be readily inferred that $E\{W_1(\kappa)\} = 0$ and $E\{W_2(\kappa)\} = 0$, therefore the mean values of $\hat{\Gamma}(\kappa)$ and $\hat{B}(\kappa)$ result in:

$$\begin{array}{c} E\left\{\hat{\Gamma}(k)\right\} = \Gamma(k), \\ E\left\{\hat{B}(k)\right\} = B(k). \end{array} \tag{28}$$

These equations mean that the proposed estimators are unbiased. Now, the variance of the estimators is to be evaluated. First, consider the variance of $\hat{\Gamma}(\kappa)$, which is defined as:

$$var\left\{\hat{\Gamma}(\kappa)\right\} = \sigma^2_{\hat{\Gamma}(\kappa)} = E\left\{\hat{\Gamma}(\kappa)^2\right\} - E\left\{\hat{\Gamma}(\kappa)\right\}^2, \tag{29}$$

where $\hat{\Gamma}(\kappa)^2 = (\Gamma(\kappa) + W_1(\kappa)S_{aN}(\kappa) + W_2(\kappa)S_{bN}(\kappa))^2$ while $E\left\{\hat{\Gamma}(\kappa)\right\}^2 = \Gamma(\kappa)^2$ from (28). Expanding the expression and distributing the expectation operator, (29) results in:

$$\begin{array}{l} \sigma^2_{\hat{\Gamma}(\kappa)} = E\left\{\Gamma(\kappa)^2\right\} + 2\zeta(\kappa)E\{(W_1(\kappa) + W_2(\kappa))\Gamma(\kappa)\} + \\ \qquad \zeta(\kappa)^2 E\left\{(W_1(\kappa) + W_2(\kappa))^2\right\} - E\{\Gamma(\kappa)\}^2, \end{array} \tag{30}$$

where $\zeta(\kappa) = \frac{S_{aN}(\kappa)+S_{bN}(\kappa)}{2}$. Knowing that $W_1(\kappa)$ and $W_2(\kappa)$ are independent random variables corresponding to different realizations of weighted noise, (30) is readily reduced to:

$$\sigma^2_{\hat{\Gamma}(\kappa)} = \sigma^2_{\Gamma(\kappa)} + \zeta(\kappa)^2\left(|\Gamma_{Rx}(\kappa)|^2 + |B_{Rx}(\kappa)|^2\right)\sigma^2_{N(\kappa)}, \tag{31}$$

where $\sigma^2_{N(\kappa)}$ is the variance of $N_x(\kappa)$, i.e. the AWGN variance. Following a similar reasoning, it can be shown that the variance of $\hat{B}(\kappa)$ is:

$$\sigma^2_{\hat{B}(\kappa)} = \sigma^2_{B(\kappa)} + \zeta(\kappa)^2\left(|\Gamma_{Rx}(\kappa)|^2 + |B_{Rx}(\kappa)|^2\right)\sigma^2_{N(\kappa)}. \tag{32}$$

Consider now that $\hat{\Gamma}_{av}(\kappa)$ and $\hat{B}_{av}(\kappa)$ are estimates obtained by averaging p training realizations, as in

$$\begin{array}{rcl} \hat{\Gamma}_{av}(\kappa) & = & \frac{1}{p}\sum_{i=1}^{p}\hat{\Gamma}_i(\kappa), \\ \hat{B}_{av}(\kappa) & = & \frac{1}{p}\sum_{i=1}^{p}\hat{B}_i(\kappa), \end{array} \tag{33}$$

where each $\hat{\Gamma}_i(\kappa)$ and $\hat{B}_i(\kappa)$ are obtained from (24); then, it can be readily seen that these estimates remain unbiased. In addition, it follows directly that the difference between the averaged estimated variance and its real value, for both $e_{\hat{\Gamma}_{av}(\kappa)}$ and $e_{\hat{B}_{av}(\kappa)}$, becomes:

$$\begin{array}{rcl} e_{\hat{\Gamma}_{av}(\kappa)} = \left(\sigma^2_{\hat{\Gamma}_{av}(\kappa)} - \sigma^2_{\Gamma(\kappa)}\right) & = & \frac{\zeta(\kappa)^2\left(\left|\Gamma_{Rx}(\kappa)^2\right| + \left|B_{Rx}(\kappa)^2\right|\right)\sigma^2_{N(\kappa)}}{p}, \\ e_{\hat{B}_{av}(\kappa)} = \left(\sigma^2_{\hat{B}_{av}(\kappa)} - \sigma^2_{B(\kappa)}\right) & = & \frac{\zeta(\kappa)^2\left(\left|\Gamma_{Rx}(\kappa)^2\right| + \left|B_{Rx}(\kappa)^2\right|\right)\sigma^2_{N(\kappa)}}{p}. \end{array} \tag{34}$$

From (34), it is obvious that $e_{\hat{\Gamma}_{av}(\kappa)} \to 0$ and $e_{\hat{B}_{av}(\kappa)} \to 0$ when $p \to \infty$. Without loss of generality, it can be considered that the norms $\left(\left|\Gamma_{Rx}(\kappa)^2\right| + \left|B_{Rx}(\kappa)^2\right|\right) = 1$ [8]. Equations in (28) and (34) demonstrate that the estimations converge at the true I/Q imbalance factors' value as the number of estimations increases, i.e., the estimators in (22) are consistent.

B. Computational complexity and PAPR

It can be seen from (22) that the complexity of the proposed algorithm is a lineal function of the number of frequency components to be estimated. Furthermore, it is remarkable that the operations involved on the estimation are very easy–to–implement in the hardware context because the Hadamard products can be reduced to sign changes and the division by 2 is matter of right bit-shifts.

In addition to the simplicity of the estimation algorithm, an extra benefit of using GCS training sequences arises from the PAPR that they exhibit. Large PAPR is one of the disadvantages of the OFDM system, and it occurs when the

TABLE I
STATE-OF-THE-ART APPROACHES PERFORMANCE COMPARISON

Algorithm	Complexity	PAPR	Operations involved	Suitable for estimation of I/Q imbalance
Proposed	$O(N)$	≤ 2	Adds, bit–shifts	FS Tx, Multipath, FS Rx and combinations
[8]	$O(N^2)$	1	Matrix–vector multiplication, Inverse matrix	FS Tx, Multipath, FS Rx and combinations
[24]	$O(N^2)$	*	Adds, Divisions	FI Tx, Multipath, FI Rx and combinations
[25]	$O(N^3)$	*	Matrix–Matrix multiplications, Inverse matrix	FS Tx, Multipath, FS Rx and combinations
Multi–tones	$O(N)$	N	Adds, bit–shifts	FS Tx, Multipath, FS Rx and combinations

* There is no PAPR analysis in this paper, therefore PA distortions could affect the estimations.

TABLE II
I/Q IMBALANCE SIMULATION PARAMETERS

Identifier	g_1	φ (degrees)	g_2	α (degrees)
c1	1.2	5	1.2	5
c2	1.2	5	0.8	−5
c3	0.8	−5	1.2	5
c4	0.8	−5	0.8	−5
c5	1	0	1	0
c6	1.2	5	1	0
c7	1	0	1.2	5

time–domain signals corresponding to the N sinusoidal sub-carriers add up constructively; this produces a peak power of as much as N times the average power. For the proposed estimators, it is well–known that the inverse DFT of the GCS are sequences having a PAPR ≤ 2 [11], [23]. This ensures that the PA will not modify the WLS modelling of the FS I/Q imbalance, making the proposed estimator reliable.

In the TABLE I it is presented a comparison between different estimation algorithms proposed in recent papers. The metrics of order of complexity $O(\cdot)$, the PAPR concerning the training sequences used in the estimation process, the operations involved and the modeled cases of I/Q imbalance are compared. The results clearly show that, aside from the fact that all the I/Q imbalance cases can be estimated by this algorithm, the best trade–off between complexity and PAPR is the one obtained by the proposed novel algorithm. The last makes this algorithm suitable for low-cost and highly reliable implementations in real RCS.

V. SIMULATIONS OVER AN OFDM SYSTEM

In this section, a general 64-QAM OFDM data transmission scheme that exhibits FS Tx I/Q imbalance, FS Rx I/Q imbalance and multipath propagation channel is simulated. Without loss of generality, the OFDM symbol is considered to contain 48 data sub–carriers, 4 pilot sub–carriers, 11 guards and DC and a proper cyclic prefix to avoid inter–symbol interference. The length of the GCS is the same as the OFDM symbol (64), however it is not planned to estimate the I/Q imbalance at DC and guards. The imbalance factors are formed by considering maximum and minimum values of gain and phase imbalances between orthogonal branches at Tx and Rx found in recent papers, as in [25]. TABLE II shows the imbalance system parameters used in the simulation.

The discrete time–domain filters that represent the imbalance between I/Q LPFs are the following: $f_{I,Tx}(n) = [1, 0.04, -0.03]$ and $f_{Q,Tx}(n) = [1, -0.04, -0.03]$ for Tx and $f_{I,Rx}(n) = [1, 0.05]$ and $f_{Q,Rx}(n) = [1, -0.05]$ for Rx [6]. For the simulation of the frequency selectivity cases, a 5–taps FIR complex filter was used. The power of these taps corresponds to the first five coefficients of the following power delay profile: $PDP(n) = \frac{1}{\alpha}e^{-n^2/2}$, where α is a normalization factor to guarantee a lossless channel. No codification or scrambling scheme was considered.

Two metrics were chosen for showing performance results of the proposed estimator: the mean squared error (MSE) between estimated and actual value of the imbalance parameters, and bit error rate (BER), which shows the system performance when the estimator is used with the pre–distortion scheme described in (7) and (9).

Before discussing performance results, it is important to verify the correctness of the theoretical results in (34). This is shown in Fig. 3, which presents several curves of the variance on the estimation of $\hat{\Gamma}_{av}(\kappa)$ with an I/Q imbalance scenario corresponding to identifier c2 in TABLE II. In addition, the Tx, Rx and channel filters mentioned before were included to test the theoretical results in a simulation scenario with the complete FS I/Q imbalance case. The identifiers Sim xdB and Theor xdB correspond to the results obtained by simulation and (34) respectively, at xdB, where x=10, 15, 20 and 25. Simulation results were obtained by averaging $20,000$ realizations of the estimation for each value of p, and choosing $\kappa = 13$. From the figure, it can be concluded that simulation and theory agree; also, the estimation error diminishes with the number of iterations and with the considered SNR value. Once the concordance of the theoretical and simulated error estimation values is reliably established, (34) can be used to pre–define the number of iterations p required to provide a confidence interval for a given SNR. In the following figures, however, the performances obtained by simulations were taken into consideration.

Fig. 4(a) and Fig. 4(b) show the measured MSE on the estimation of $\hat{\Gamma}(k)$ and $\hat{B}(k)$ respectively, for all identifiers in TABLE II under the FS Tx/Rx I/Q imbalance scenario. The results were obtained by averaging 150 estimation realizations and $p = 8$. The figure shows, as expected from previous discussions, that the MSE diminishes with the SNR value. Note also that the proposed estimator works well for all extreme cases under consideration, and that the achieved error is not too different between them.

Fig. 5(a) and Fig. 5(b) consider the FI Tx/Rx I/Q imbalance scenario, where the FIR filters for the imbalance within I/Q LPFs and the multipath channel are taken into account. Again, 150 estimation realization were averaged, $p = 8$ and all identifiers in TABLE II were included. The results show that the worst scenarios of I/Q imbalance can be properly estimated by the proposed algorithm. In fact, note that after a few dBs of SNR, the achieved MSE in both FS and FI cases,

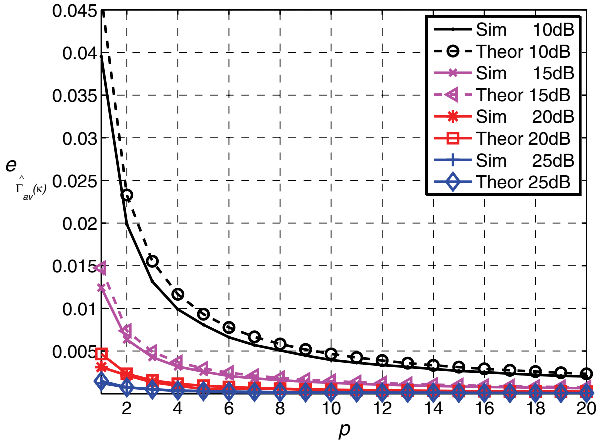

Fig. 3. Comparison between the measured error variance and the theoretical error variance in (34) for the estimation of $\hat{\Gamma}_{av}(\kappa)$ when p averaged estimations are performed for SNR=[10,15,20,25]dB and $\kappa = 13$.

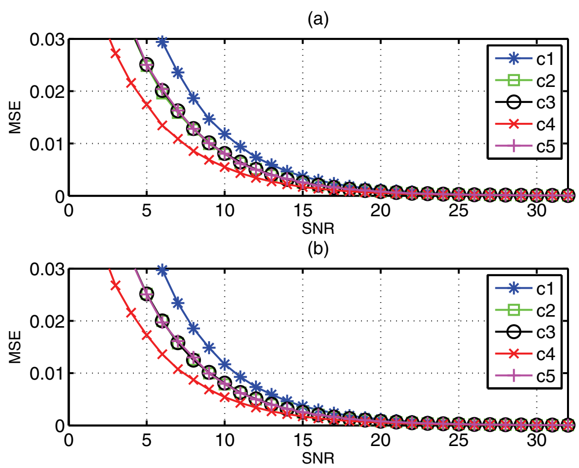

Fig. 4. MSE in the estimation of a) $\hat{\Gamma}_{av}(\kappa)$ and b) $\hat{B}_{av}(\kappa)$ when a FS I/Q imbalance scenario is considered and whose parameters are defined by identifiers c1 - c5 in TABLE II for $p = 8$ averaged estimations.

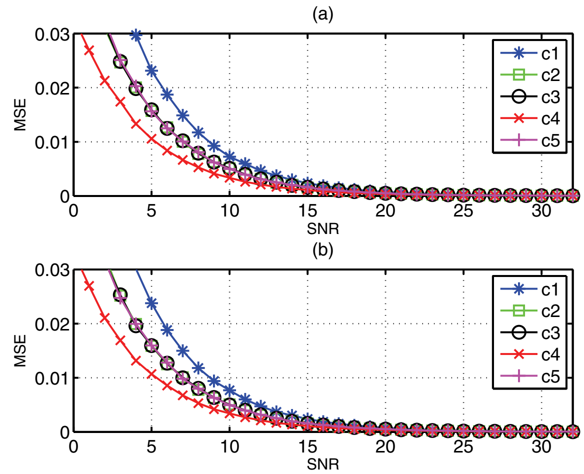

Fig. 5. MSE in the estimation of a) $\hat{\Gamma}_{av}(\kappa)$ and b) $\hat{B}_{av}(\kappa)$ when a FI I/Q imbalance scenario is considered and whose parameters are defined by identifiers c1 - c5 in TABLE II for $p = 8$ averaged estimations.

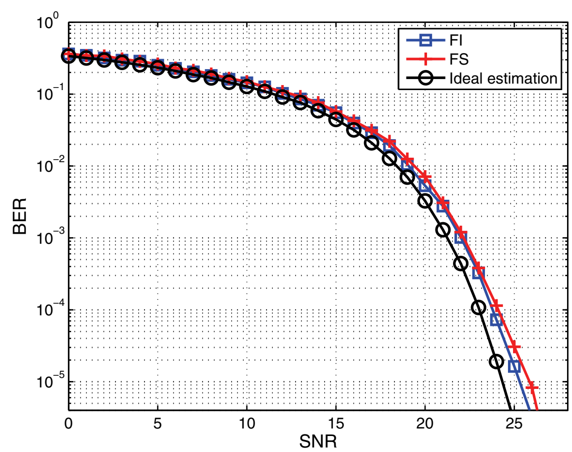

Fig. 6. BER obtained under I/Q imbalance simulation parameters defined as case c6 in TABLE II and $p = 8$ averaged estimations.

is practically the same.

Fig. 6, Fig. 7 and Fig. 8 show the BER performance of a system transmitting a 64–QAM constellation with imbalance parameters defined in identifier c6, c7 and c1 in TABLE II, respectively. Fig. 6 considers imbalances only at the Tx side, Fig. 7 considers imbalance only at the Rx side while Fig. 8 includes imbalances at both sides of the link. In each figure, three scenarios are considered: FI, FS and the case of an ideal I/Q imbalance estimation. All cases use the compensation scheme introduced in (9). From the figures, it can be noted that the BER results, when using the proposed estimator, are practically the same as those obtained with complete knowledge of imbalance parameters for all the cases. In fact, the difference is less than 1dB and quite close to well–known ideal performance (a system without I/Q imbalances or multipath).

VI. Conclusion

The I/Q imbalance problem can be modeled with a WLS structure. This model can include all the imbalance parameters: gain imbalances, phase imbalance, LPF differences at both the Tx and Rx sides and the propagation channel. By making use of a different interpretation of the GCS properties, a novel trained estimation algorithm has been proposed. This estimator has the important statistical feature of consistence. In addition, the variance of the error in the estimation of the WLS parameters has a closed and verified form, allowing the number of averaged estimations p to be predefined according to the desired system performance. Besides these important statistical features, the proposed algorithm exhibits a very low complexity of $O(N)$ and requires only sign changes, complex adds and right bit–shifts to the BB received signal in the frequency domain. An additional advantage is that the PAPR of the inverse DFT of the GCS makes it possible to consider that the PA is not introducing non-linearities into the estimation process; hence, this problem can be addressed separately. The achieved MSE and BER performance suggest that the proposed algorithm can be successfully implemented in practical applications.

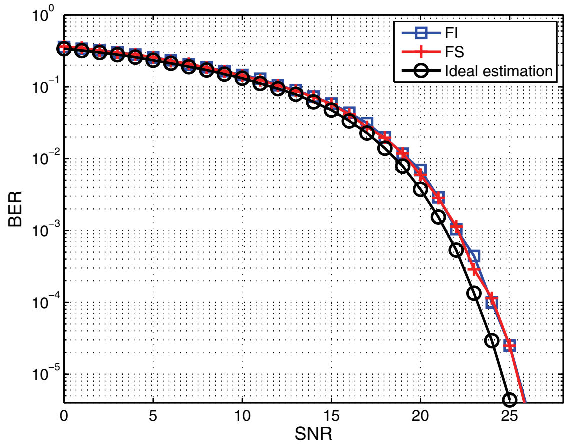

Fig. 7. BER obtained under I/Q imbalance simulation parameters defined as case c7 in TABLE II and $p = 8$ averaged estimations.

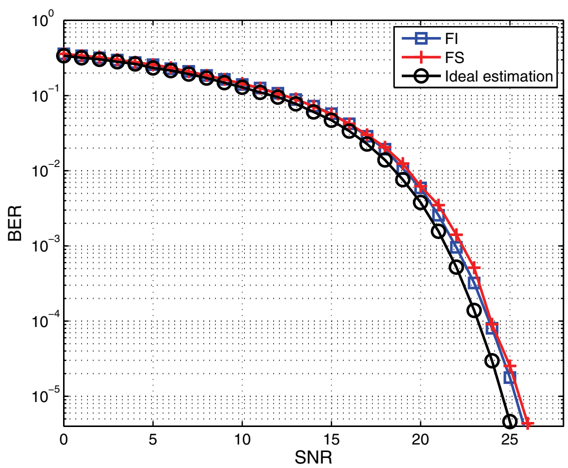

Fig. 8. BER obtained under I/Q imbalance simulation parameters defined as case c1 in TABLE II and $p = 8$ averaged estimations.

References

[1] Y.-H. Chung and S.-M Phoong, "Joint estimation of I/Q imbalance, CFO and channel response for MIMO OFDM systems," *IEEE Trans. Commun.*, vol. 58, no. 5, pp. 1485–1492, May 2010.

[2] D. Tandur and M. Moonen, "Efficient compensation of transmitter and receiver IQ imbalance in OFDM systems," *EURASIP J. Advances Signal Process.*, vol. 2010, Article ID 106562, 14 pages, 2010.

[3] J. Tubbax, B. Come, L. Van der Perre, S. Donnay, M. Engels, Hugo De Man, and M. Moonen, "Compensation of IQ imbalance and phase noise in OFDM systems," *IEEE Trans. Wireless Commun.*, vol. 4, no. 3, pp. 872–877, May 2005.

[4] J. C. Oostveen, A. Schoonen, and F. Willems, "Baseband compensation of transmitter and receiver IQ imbalance for OFDM in frequency selective fading channels," in *Proc. 2006 IEEE Workshop Signal Process. Advances Wireless Commun.*, pp. 1–5.

[5] L. Anttila, M. Valkama, and M. Renfors, "Frequency-selective I/Q mismatch calibration of wideband direct-conversion transmitters," *IEEE Trans. Express Briefs*, vol. 55, no. 4, pp. 359–363, Apr. 2008.

[6] Y. Zou, M. Valkama, and M. Renfors, "Analysis and compensation of transmitter and receiver I/Q imbalances in space-time coded multi-antenna OFDM systems," *EURASIP J. Wireless Commun. Netw.*, 2008, Article ID 391025, 16 pages, 2008.

[7] T. C. W. Schenk, P. F. M. Smulders, and E. R. Fledderus, "Estimation and compensation of frequency selective TX/RX IQ imbalance in MIMO OFDM systems," in Proc. *2006 IEEE International Conf. Commun.,* vol. 1, pp. 251–256.

[8] I. A. Arriaga-Trejo, A. G. Orozco-Lugo, A. Veloz-Guerrero, and M. E. Guzman, "Widely linear system estimation using superimposed training," *IEEE Trans. Signal Process.*, vol. 59, no. 11, pp. 5651–5657, Nov. 2011.

[9] G. Xing, M. Shen, and H. Liu, "Frequency offset and I/Q imbalance compensation for direct-conversion receivers," *IEEE Trans. Wireless Commun.*, vol. 4, no. 2, pp. 673–680, Mar. 2005.

[10] Y.-H. Chung and S.-M. Phoong, "Channel estimation in the presence of transmitter and receiver I/Q mismatches for OFDM systems," *IEEE Trans. Wireless Commun.*, vol. 8, no. 9, pp. 4476–4479, Sept. 2009.

[11] J. Davis and J. Jedwab, "Peak-to-mean power control in OFDM, Golay complementary sequences and Reed-Muller codes," *IEEE Trans. Inf. Theory*, vol. 45, pp. 2397–2417, Nov. 1999.

[12] M. Nazarathy, S. A. Newton, R. P. Giffard, D. S. Moberly, F. Sischka, and W. R. Trutna Jr., "Real-time long range complementary correlation optical time domain reflectometer," *IEEE J. Lightwave Technol.*, vol. 7, no. 1, pp. 24–38, 1989.

[13] B. J. Seberry, B. J. Wysocki, and T. Wysocki, "Golay sequences for DS CDMA applications," in *Proc. 2002 Int. Symp. DSP Commun. Syst.*, pp. 103–108.

[14] A. V. Alejos, M. G. Sanchez, and I. Cuinas, "Improvement of wideband radio channel swept time-delay cross-correlation sounders by using Golay sequences," *IEEE Trans. Veh. Technol.,* vol. 56, no. 1, pp. 362–368, Jan. 2007.

[15] B. Picinbono and P. Chevalier, "Widely linear estimation with complex data," *IEEE Trans. Signal Process.*, vol. 43, no. 8, pp. 2030–2033, Aug. 1995.

[16] T. R. Qureshi, M. D. Zoltowski, and R. Calderbank, "Target detection in MIMO radar in the presence of Doppler using complementary sequences," in *Proc. 2010 IEEE International Conf. Acoustic, Speech Signal Process.*, pp. 2766–2769.

[17] "IEEE standard for Information technology-Telecommunications and information exchange between systems-Local and metropolitan area networks-Specific requirements. Part 15.3: Wireless Medium Access Control (MAC) and Physical Layer (PHY) Specifications for High Rate Wireless Personal Area Networks (WPANs). Amendment 2: Millimeter-wavebased Alternative Physical Layer Extension," IEEE Std 802.15.3c-2009 (Amendment to IEEE Std 802.15.3-2003), pp. c1187, Oct. 12 2009.

[18] J. Chen, S.-P. Chen, Z.-D. Qin, and T.-F. Wang, "A new scheme of coded ultrasound using Golay codes," *J. Zhejiang University - Science C.*, pp. 476–480, 2010.

[19] V. P. G. Jimenez, M. S. Fernandez, and A. G. Armada, "Study and implementation of complementary Golay sequences for PAR reduction in OFDM signals," in *Proc. 2002 Mediterranean Electrotechnical Conf.*, pp. 198–203.

[20] V. Braun, "Golay sequences for identification of systems with weak nonlinear distortion," *IEE Proc. Science, Measurements Technol.*, vol. 45, no. 3, pp. 123–128, May 1998.

[21] M. Golay, "Complementary series," *IRE Trans. Inf. Theory*, vol. 7, no. 2, pp. 82–87, Apr. 1961.

[22] S. Kay, *Fundamentals of Statistical Signal Processing.* Prentice Hall, 1993.

[23] C. Vee Chong, R. Venkataramani, and V. Tarokh, "A new construction of 16-QAM Golay complementary sequences," *IEEE Trans. Inf. Theory*, vol. 49, pp. 2953–2959, Nov. 2003.

[24] A. Tarighat and A. H. Sayed, "Joint compensation of transmitter and receiver impairments in OFDM systems," *IEEE Trans. Wireless Commun.*, vol. 6, no. 1, pp. 240–247, Jan. 2007.

[25] L. He, S. Ma, Y.-C. Wu, Y. Zhou, T.-S. Ng, and H. V. Poor, "Pilot-aided IQ imbalance compensation for OFDM systems operating over doubly selective channels," *IEEE Trans. Signal Process.*, vol. 59, no. 5, pp. 2223–2233, May 2011.

R. Rodríguez–Ávila was born in San Pedro de las Colonias, Coahuila, México, in 1984. In 2007, he received the B.Sc. degree in Electronic Engineering from Instituto Tecnológico de Veracruz, Veracruz, México and the M.Sc. degree in Electrical Engineering, specializing in Telecommunications, from CINVESTAV–IPN, Guadalajara, Jalisco, México in 2010. Currently, he is working in getting his Ph.D. degree in CINVESTAV–IPN, Guadalajara. His research interests include digital signal processing, modeling, base–band characterization and estimation/compensation of non idealities in the analog section of radio communication systems.

G. Núñez–Vega was born in Ciudad Obregon, Sonora, México in 1988. He received the B. Sc. in Electronic Engineering from Instituto Tecnológico de Sonora (ITSON) in 2010 and the M. Sc. degree in Electrical Engineering with specialization in Telecommunications from CINVESTAV-IPN, Guadalajara, México in August 2012. Since September 2012, he has been working as a design engineer for CINVESTAV-IPN.

R. Parra-Michel (S97M04) was born in Guadalajara City, Mexico, in 1973. He received the B.Sc. degree in Electronics and Communications from University of Guadalajara, Jalisco, Mexico, in 1996, the M.Sc. degree in Electrical Engineering, specializing in Communications, from CINVESTAV-IPN, Guadalajara, Mexico, in 1998 and the Ph.D. degree in Electrical Engineering specialized in digital signal processing for communications from CINVESTAV-IPN, Mexico City, in 2003. He has collaborated with several companies and institutions either in academic or technology projects, such as Siemens, Lucent, Mabe, Mixbaal, Hewlett-Packard and Intel. He is currently a full member of research staff at CINVESTAV-IPN in Guadalajara Unit. His research interests include modeling, simulation, estimation and equalization of communication channels, and digital implementation of DSP algorithms for communication systems.

A. Mendez–Vazquez is a researcher professor at Cinvestav Guadalajara. He got his Ph.D. degree in computer engineering at the University of Florida, Gainesville, Florida in 2008. He received his Master of Sciences degree in Computer and Information Science and Engineering at the University of Florida, Gainesville, Florida in 2002. He got his Bachelor degree in Mathematics at the University of Yucatan, Merida, Yucatan in 1999. His research interests include optimization and multi-objective optimization, statistical methods for machine learning, and fuzzy measures and Choquet integration.